J Food Sci Technol
https://doi.org/10.1007/s13197-019-03948-7

ORIGINAL ARTICLE

Evidence on the discrimination of quinoa grains with a combination of FT-MIR and FT-NIR spectroscopy

Silvio D. Rodríguez[1,2] · M. P. López-Fernández[1,2] · S. Maldonado[1,2] · M. P. Buera[1]

Revised: 22 June 2019 / Accepted: 11 July 2019

Abstract Quinoa is considered as a valuable re-emergent crop due to its nutritional composition. In this study, five quinoa grains from different geographical origin (Real, CHEN 252, Regalona, BO25 and UDc9) were discriminated using a combination of FT-MIR and FT-NIR spectra as input for principal component analysis (PCA), cluster analysis (CA) and soft independent modelling class analogy (SIMCA). The results obtained from PCA and CA show a great power of discrimination, with an average silhouette width value of 0.96. Moreover, SIMCA showed an error rate and accuracy values of 0 and 1 respectively with only 4% misclassified samples. A relationship between each principal component and the most important variables for the discrimination were mainly due to vibrations of several oleofins groups (C–H, C–H_2, C–H_3), alkene group (–CH=CH–), hydroxyl group (O–H) and Amides I and II vibrational modes.

Keywords Infrared spectroscopy · Near infrared spectroscopy · Quinoa grains · Chemometric methods

Introduction

According to archaeological records, quinoa was domesticated in the basin of the Titicaca Lake 5000 years ago (Bazile and Baudron 2015). Its cultivation was extended throughout the central and north-central Andean valleys and southwards into the Araucanian coastal region and adjacent Patagonia, diversifying into its five principal ecotypes: Altiplano, Salares, Inter-Andean valleys, Coastal and Yunga (Jellen et al. 2015).

Quinoa is considered a crop with a large variability adapted to many agro-climatic habitats and edaphic conditions, including stress conditions like drought, frost and or soil with high salinity (Bhargava et al. 2007; Nascimento et al. 2014). During years, quinoa was rejected as being considered indigenous food. However, during the second half of the twentieth century it was rediscovered and revalorized due to its great nutritional benefits mainly related to the aminoacidic profile (Bazile and Baudron 2015). Quinoa is a grain, but it is considered a pseudocereal, as amaranth, buckwheat and chia among others, because it does not belong to Gramineae family. Quinoa grain is rich in both macronutrients (proteins, polysaccharides and fats) and some micronutrients (polyphenols, vitamins and minerals) (Nascimento et al. 2014). However, these nutrients may significantly differ in different cultivars or genotypes (Abderrahim et al. 2015; Tang et al. 2015). Despite its potential, quinoa is still an underutilized crop, with few active breeding programs and breeding efforts are needed to improve the crop for important agronomic traits to expand production worldwide (Jarvis et al. 2017).

In recent years, consumers have shown greater interest in the relationship between food intake and health, prioritizing foods with nutritional benefits. Due to this fact, the focus has been placed on foods with high nutritional value such as

Electronic supplementary material The online version of this article (https://doi.org/10.1007/s13197-019-03948-7) contains supplementary material, which is available to authorized users.

✉ Silvio D. Rodríguez
silviodavidrodriguez@gmail.com

[1] Facultad de Ciencias Exactas y Naturales, Universidad de Buenos Aires, Buenos Aires, Argentina

[2] Instituto de Biodiversidad y Biología Experimental y Aplicada (IBBEA), CONICET – Universidad de Buenos Aires, Intendente Güiraldes 2160, Pabellón 2, 4to Piso, Ciudad Universitaria, Buenos Aires, Argentina

Published online: 23 July 2019

quinoa grains or their derivatives (Liutho et al. 2016). This increase in demand meant that the prices of quinoa grains and flour increased in several countries, also increasing the risk of possible adulterations, requiring rapid and efficient analytical techniques for their detection. Accordingly, many efforts have been made to characterize and discriminate quinoa grains or quinoa products by their geographical origin (Ruiz et al. 2014). The use of quinoa seeds to produce food ingredients requires a rapid and efficient analysis for their characterization and/or origin classification according to possible variations on their nutrient profile. Moreover, during the production of food ingredients made of quinoa, there are risks of contamination with other seeds or cereals. Thus, innovative analytical methods are necessary for a better understanding and characterization of quinoa grains, which have also many interesting functional properties.

The techniques used to characterize different components from different cultivars of cereal or pseudo-cereal flours are Fourier Transform Infrared (FT-IR) spectroscopy in the mid (450–4000 cm^{-1}, FT-MIR) and near ranges (4000–10,000 cm^{-1}, FT-NIR). FT-NIR has been combined with robust multivariate statistics for determination of dietary constituents (moisture, protein, fat, ashes and carbohydrates) in cereal and pseudo-cereal grains from different ecotypes and cultivars (Pojić et al. 2008; González Martín et al. 2014; González-Muñoz et al. 2016; Encina-Zelada et al. 2017). Moreover, joint FT-MIR and FT-NIR studies have been used to determine antioxidant capacity of vegetables (Li et al. 2015). Spectroscopic results are enhanced in a greater way when used in combination with multivariate statistical methods also known as chemometric methods, in which each measurement is associated with multiple variables (Van den Berg et al. 2013). Spectroscopic data consist in many variables, which are the intensities associated to the frequency or wavelength of each obtained spectrum. These variables are highly correlated and could contain systematic variations and chemometric methods are used to reduce the negative impact of these (Gislum et al. 2004; Kim and Kays 2009). The aim of the present work was to explore the FT-MIR and FT-NIR to discriminate among different quinoa grains from diverse geographical areas using different chemometric approaches, such as, pattern recognition tools. To the best of our knowledge, quinoa grain discrimination according to their geographical origin has been not studied using FT-IR and chemometrics.

Materials and methods

Materials

Ten independent samples of five quinoa (*Chenopodium quinoa* Willd.) grains from five different geographical areas were analyzed: CHEN 252 from Maimará, Jujuy, Argentina (Inter-Andean valley ecotype), BO25, UDc9 and Regalona from three different Chilean localities (Coastal ecotype) and Real from Postosi, Bolivia (Altiplane ecotype) were grown in a chamber under controlled conditions 16 h light/8 h dark cycles at 25 °C and grains were collected. Quinoa grains were mortared previous to spectroscopic analysis and passed through a sieve with a mesh of 420 μm.

Methods

Fourier transform mid infrared spectra (FT-MIR)

The FT-MIR spectra were recorded using a FT-IR spectrometer (Spectrum 400, Perkin Elmer Inc., Shelton CT, USA) equipped with an attenuated total reflectance (ATR) accessory (PIKE technologies, Inc. Madison, WI, USA). Each sample was placed over the ATR crystal (one reflectance, incident angle of 45°) and the spectrum was recorded from 600 to 4000 cm^{-1} using a resolution of 4 cm^{-1} and an accumulation of 64 scans. All the spectra were base-line corrected and normalized (Spectrum Software ver. 6.3, Perkin Elmer, Inc.) before chemometric analysis. Due to strong crystal absorbance, signals from 1800 to 2500 cm^{-1} were not considered for further analysis.

Fourier transform near infrared spectra (FT-NIR)

The samples were scanned in the same FT-IR spectrometer mentioned above. Each powdered sample was put into a glass recipient until it covered the bottom, the recipient with the sample was placed over the integrating sphere accessory and scanned from 4000 to 10,000 cm^{-1} with a resolution of 4 cm^{-1} until 64 scans were averaged. The resultant spectra were base-line corrected and normalized using Spectrum Software ver. 6.3 (Perkin Elmer, Inc.) before application of chemometric methods.

Principal component analysis

Principal component analysis (PCA) is a statistical procedure for determining similarities among the objects in a data set (e.g. samples by wavelengths). To this end, the relative locations of the samples on the most important principal components (the new, latent variables in the new space) in a two- or three-dimensional plot are compared (Jolliffe 2002).

Another outcome from the PCA method is the loading matrix, that includes information of the most relevant wavenumbers (from FTIR) for grouping the samples by their similarity. In the present work, PCA on the covariance

matrix were performed using Infostat/p2011 software (Di Rienzo et al. 2011) over FT-MIR and FT-NIR normalized spectra using absorbance units. Pareto test on the scree plot from PCA was used to select the relevant number of components.

Cluster analysis (K-means method)

Using partitioning cluster analysis (CA), or k-means cluster analysis, a set of objects (like PCA) is assigned to two or more groups (i.e., clusters), specified previously by the user, in such a way objects belonging to the same cluster are more similar to each other than objects belonging to different clusters (Johnson and Wichern 2002). As a result of the CA a clusterization vector was obtained, which indicates the assignment of each sample to a cluster. Additionally, a goodness of fit value, the average silhouette width (ASW) was obtained. ASW varies from − 1 to 1 and must be greater than 0.75 for a good assignment of the samples to the clusters (Kaufman and Rousseeuw 1987). K-means cluster analysis was performed over FT-IR data using the Infostat/p2011 software (Di Rienzo et al. 2011).

Soft independent modelling class analogy (SIMCA)

SIMCA is a learning method based on principal component and models a PCA for each class (each class correspond to a geographical origin of quinoa seeds). The resulting components are used to set classification boundaries and the assignment for each new observation can be done. The so-called Coomans plot, showing the distances for each sample and the boundaries is obtained and a sample could be either included into a class or even not assigned to any class. For this reason, SIMCA is considered a soft model (Vanden Branden and Hubert 2005; Luna et al. 2016). Moreover, a confusion matrix is calculated based on the number of well and misclassified samples. Then, additional performance parameters are obtained from the confusion matrix, such as, sensitivity (SEN), specificity (SPEC), precision (PREC) for each class and global performance parameters like accuracy (ACC), error and non-error rates (ER and NER). SEN represents the rate of correctly recognized samples to a class and is calculated as TP/(TP + FN), where TP is the number of positive cases correctly classified and FN are the false negative assignments. SPEC represents the percentage that rejects samples of all other classes and is calculated as TN/(FP + TN), where TN is the number of negative cases correctly classified and FP are the false positive assignations. PREC represents the ability to avoid wrong predictions in that class and is defined as TP/(TP + FP). SEN, PREC and SPEC values vary between 1 and 0, representing a perfect classification and no class discrimination, respectively. ACC represents the rate of false and positive samples correctly classified among all positive and negative samples and is calculated as (TP + TN)/(TP + TN + FP + FN). NER is the average value of the sensitivity for all the classes, and ER = 1 − NER. NER and ACC parameters take values from 0 to 1, indicating a perfect classification when the values are 1. ACC, NER and ER are considered global parameters giving information of the overall classification for each algorithm step (calibration or validation) (Ballabio et al. 2018).

In the present work, SIMCA was performed with the Classification Toolbox (Ballabio and Consonni 2013) under GNU Octave language. The cross-validation step selected for SIMCA was venetian blinds using 10 groups.

Results and discussion

FT-MIR spectra

The shape of the spectra for the five quinoa grains studied only revealed differences in the relative intensities of absorption bands. Each band could be associated to different vibrational modes of the molecular moieties present in the grain components. Figure 1 shows normalized FT-MIR spectra, in absorbance units, for one representative replicate of each quinoa grain samples. In the five spectra the following absorption bands could be detected. A broad absorption band from 3010 to 3750 cm^{-1}, due to O–H stretching mainly associated carbohydrates and moisture (Kizil et al. 2002). Moreover, a band is observed from 2800 to 3000 cm^{-1} (with two overlapped peaks), typically associated to C–H and C–H_2 symmetric and asymmetric stretching, and a band with a maximum of 1745 cm^{-1} (stretching of the ester carbonyl group) are mainly

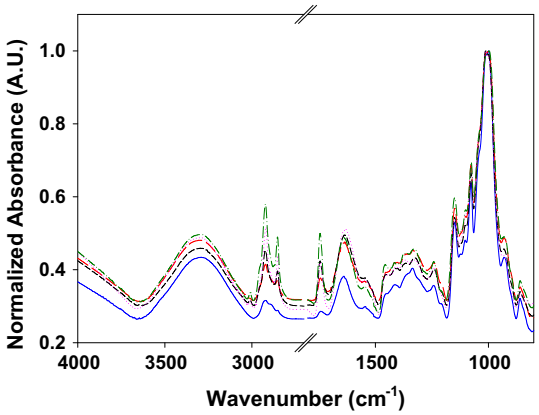

Fig. 1 FT-MIR normalized spectra of one replicate of the five types of quinoa grains measured: Real (solid blue line), CHEN 252 (long dash red line), Regalona (short dash black line), BO25 (dotted pink line) and UDc9 (dash-dot green line) (color figure online)

attributed to the lipidic components of the grains (Roa et al. 2014). The signals mainly associated to proteins bonds (Amide I and II) are shown with maxima at 1640 cm^{-1} and 1540 cm^{-1} (Barth 2007; Guzman-Ortiz et al. 2014). Additionally, a small broad band from 1200 to 1500 cm^{-1} is represented by CH_2OH side chain related mode, C–O–H bending, C–H_2 twisting, C–H_2 bending and C–O–O stretch. Spectra also show a strong absorption band, from 900 to 1200 cm^{-1} due to C–O and C–C stretching (1163 cm^{-1}), C–O–H bending (1094 cm^{-1}) and C–H bending (1067 cm^{-1}). Finally, below 900 cm^{-1}, quite small bands can be observed due to skeletal modes of the pyranose ring (Kizil et al. 2002; Capron et al. 2007; Warren et al. 2016).

FT-NIR spectra

Figure 2 shows the normalized FT-NIR spectra, in absorbance units, for each type of quinoa grain studied. The spectra obtained for the five different origins were similar, with slight differences, showing bands with maxima at 8330 cm^{-1} (C–H second overtone of –CH_2, –CH_3, –CH=CH–), 6875 cm^{-1} (O–H first overtone), 5705 cm^{-1} (C–H stretching first overtone), 5170 cm^{-1} (O–H stretching and deformation), 4745 cm^{-1} (C–H stretching and deformation, O–H stretching and C–O deformation of carbohydrates), 4325 cm^{-1} (C–H stretching and C–H deformation of –CH_2 and –CH_3) (Li et al. 2015; Lohumi et al. 2015 and references therein).

Application of principal component analysis and cluster analysis to FT-IR spectra

Initially, in an exploratory analysis, FT-MIR and FT-NIR spectra were provided separately as input data for PCA showing a poor discrimination of the grains. However, the use of both (FT-MIR and FT-NIR) as input variables

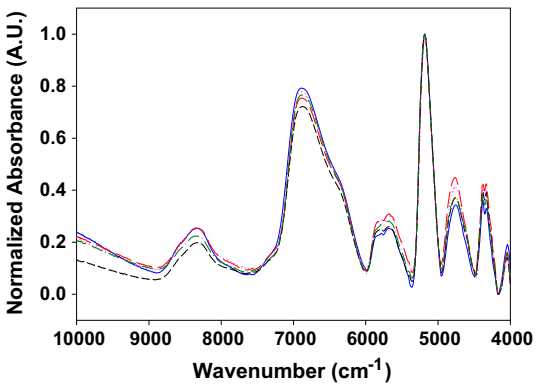

Fig. 2 FT-NIR normalized spectra of one replicate of the five types of quinoa grains measured: Real (solid blue line), CHEN 252 (long dash red line), Regalona (short dash black line), BO25 (dotted pink line) and UDc9 (dash-dot green line) (color figure online)

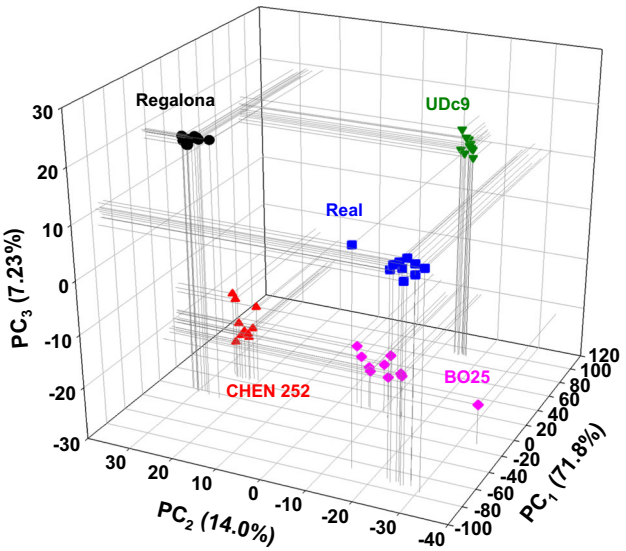

Fig. 3 3D scatter plot of the three first components obtained as outcomes from PCA of FT-MIR and FT-NIR spectra: Real (blue squares), CHEN 252 (red triangles up), Regalona (black circles), BO25 (pink diamonds) and UDc9 (green triangles down). In brackets are the variance amounts associated with each component (color figure online)

together, provided a good grouping pattern according similarities, and promote the use of further PCA-based methods, such as SIMCA. Figure 3 shows the three-dimensional score plot (3D-PCA-plot, PC_1 vs. PC_2 vs. PC_3) considering the first three components from PCA, each dot of this figure is an independent sample of quinoa from five different geographical areas measured in both FT-MIR and FT-NIR. The recovered cumulative total variance associated to the three first principal components (PC_1, PC_2 and PC_3) was 93.0%. This indicate a good amount of sample's variability explained by PCA. The pattern observed exhibit a clear grouping of the samples according similar characteristics of the quinoa grains into five groups, corresponding to the five geographical areas (Real, CHEN 252, Regalona, BO25 and UDc9).

In addition, to validate the outcomes from PCA, a cluster analysis was performed considering the original variables (FT-MIR and FT-NIR spectra) and the first three principal components as input. The results agree with those observed in Fig. 3, obtaining a clear discrimination for five groups (see cluster ID in Table SM2 in the supplementary material section), with an ASW of 0.96 (see Figure SM10 in supplementary material section). The result obtained using cluster analysis confirmed the grouping pattern observed in PCA, which implies similarities of the quinoa grains from the different geographical areas.

Table 1 shows the loadings for the first three components from PCA, indicating which of the frequencies had more influence on the discrimination of the quinoa grains. The three principal components (PC_1, PC_2 and PC_3) are

Table 1 Original variables (wavenumbers) from PCA with more impact on the first three principal components and the vibrational modes associated with

Principal component	Order of relevance[a] (#)	Wavenumber (cm^{-1})		Associated to
		Band (from–to)	Maximum at	
PC_1	1	2870–2990	2920	C–H and C–H_2 symmetric and asymmetric stretching
	2	2800–2870	2855	C–H and C–H_2 symmetric and asymmetric stretching
	3	7915–8890	8330	C–H second overtone of –CH_2, –CH_3 and –CH=CH–
	4	6625–7255	6875	O–H first overtone
	5	4245–4495	4325	C–H stretching and C–H deformation of –CH_2 and –CH_3
PC_2	1	1700–1770	1745	Stretching of the ester carbonyl groups
	2	2870–2990	2920	Described above
	3	2800–2870	2855	Described above
	4	4245–4495	4325	Described above
	5	4970–5390	5170	O–H stretching and deformation
PC_3	1	4245–4495	4325	Described above
	2	1490–1570	1540	C–N stretching, C–O stretching and C–C stretching (Amide II)
	3	4970–5390	5170	Described above
	4	1570–1705	1640	C=O stretching and N–H bending (Amide I)
	5	5380–5990	5705	C–H stretching first overtone

[a]The order of relevance of each principal component to each original variable (frequencies) was found after calculating the modulus of each loading value for each component and sorting that values from the highest to the lowest

highly influenced by both, FT-MIR and FT-NIR variables (wavenumbers). In the case of PC_1, the influence was mainly due to vibrations of several oleofin groups (C–H, C–H_2, C–H_3), alkene group (–CH=CH–) and hydroxyl group (O–H). Moreover, PC_2 is influenced by stretching of the ester carbonyl groups, vibration s of oleofin groups (C–H, C–H_2 and C–H_3) and hydroxyl (O–H) stretching and deformation. Finally, the third principal component is influenced again by vibrations of oleofin groups (C–H, C–H_2, C–H_3), hydroxyl (O–H) stretching and deformation, Amides I and II. The overtone bands associated with O–H from FT-NIR spectra (6625–7255 cm^{-1} and 4970–5390 cm^{-1}) were also found to exert a high impact on the discrimination of wheat samples (Ziegler et al. 2016).

Application of soft independent modelling class analogy (SIMCA) to FT-IR spectra

To confirm the outcomes observed using PCA and CA the data set was used to model a chemometric method for classification. SIMCA was run using 2 components for each class previously optimized with cross-validation error rate. The cumulative variance associated with those two components were 95, 93, 99, 99, and 99% for the five geographical origins respectively (Real, CHEN252, Regalona, B025 and UDc9) indicating a great amount of the data variance captured by SIMCA. Table SM1 (see *Supplementary material section*) shows the confusion matrix (also known as contingency table) obtained in the validation step, in which, each row of the matrix represents the real classes for the samples and each column represents the assigned classes using SIMCA. Only two samples from class CHEN252 were not assigned to any class. In this study SEN, SPEC and PREC showed high values (1.00) for all the classes. ER, NER and ACC values were 0, 1.00 and 1.00 respectively in agreement with the good parameters obtained for each class. In this case only two samples out of fifty were not assigned to any class, both belonging to class CHEN 252 and the percentage of not-assigned samples was 4%. Figure 4 shows the Coomans plot obtained for class Real versus class CHEN252, representing the normalized distances for each sample into the scatter plot. This plot is divided into four areas or squares by two straight lines (threshold boundaries). The plot (Fig. 4) shows a zone for the samples assigned to class Real (red dots), another zone for the samples of class CHEN252 (blue dots), a large square with all the other samples and an empty square in the case a sample was misclassified between both classes. SIMCA showed no errors in the assignment of the samples in the training step for class Real versus class CHEN252 and for the all other classes (Figures SM1 to SM9 provided in Supplementary material section). Finally, to confirm the good classification results, receiver operating characteristic curves (ROC) for all the classes in the training step were provided in the Fig. 5.

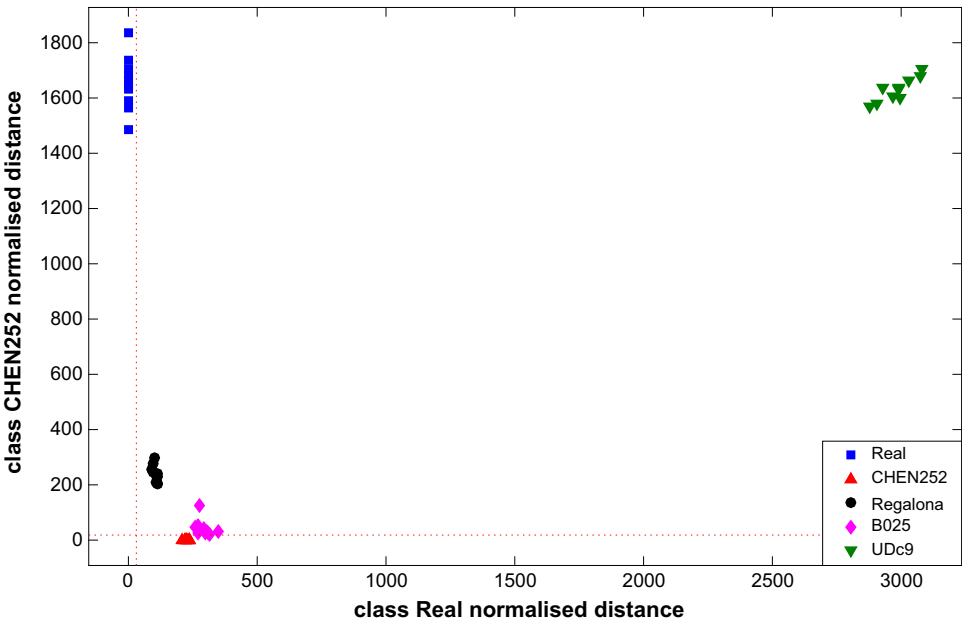

Fig. 4 Coomans plot of the class Real versus the class CHEN252 obtained from SIMCA training step

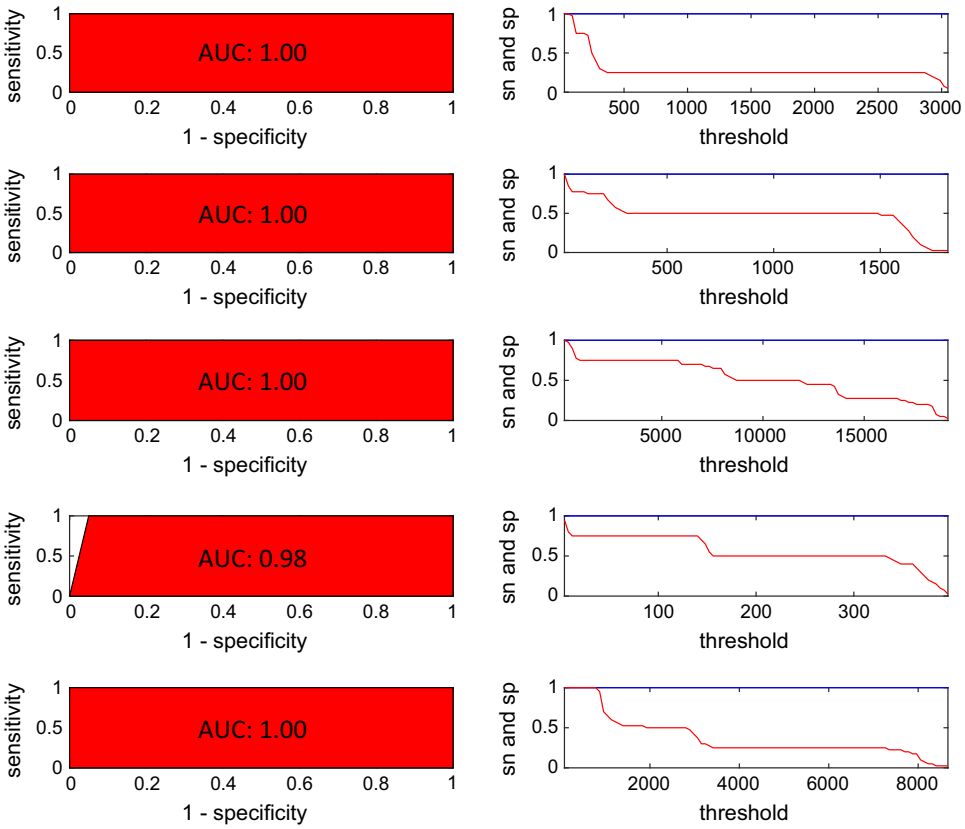

Fig. 5 ROC curves of the classes Real, CHEN252, Regalona, B025 and UDc9 from top to bottom respectively. SEN is represented with the blue line and SPEC with the red line (color figure online)

ROC curves show two plots, the plot on the right, is a plot of SEN and SPEC values varying the threshold limit (boundary limit of the class), where the optimal threshold is the value showing the highest SEN and SPEC values. The area under the plot of the left (AUC) is close to 1 when the model shows maximum classification ability and in this work were 1.00 for classes Real, CHEN252, Regalona and UDc9 and 0.98 for class B025. Recovered AUC were in good agreement to the values of the parameters found using the confusion matrix after running SIMCA algorithm (SEN, SPEC, PREC, ER and ACC). These results were in a good agreement with two others found in literature for

other grains. FT-NIR in combination with SIMCA was used by Ye et al. (2008) to classify with excellent result different botanical cornstover fractions and by Miralbés (2008) for discrimination of wheat cultivars.

Conclusion

The use of quinoa grains requires rapid and efficient analytical techniques for their characterization and classification. The observations and procedures proposed in this work demonstrate the potential capacity of the joint FT-MIR and FT-NIR analysis using chemometric methods to discriminate among five quinoa varieties. Principal component analysis and cluster analysis were a good option as a rapid discrimination tool using FT-MIR and FT-NIR spectra as input data when compared to the results of each FT-MIR and FT-NIR separate analysis. The differences observed in PCA and confirmed by CA could be mainly attributed to origin regions of the quinoa components. Additionally, SIMCA showed an excellent performance with a very low of not-assigned samples (only 4%). This analysis provided an innovative, rapid and powerful tool for investigating/discriminating the quinoa grains from different origins. Such kind of tools are necessary for a better characterization of this re-emerging food source which has many attracting nutritional and functional properties, defining adequately their potential applications and avoiding the risk of adulterations.

Acknowledgements SDR, MPLF, SM and MPB are research staff members of the National Scientific and Technical Research Council (*CONICET*). The authors are grateful for the financial support given by PICT 2013-1331 and UBACYT 2014-2017 20020130100443BA funds.

References

Abderrahim F, Huanatico E, Segura R, Arribas S, Gonzalez MC, Condezo-Hoyos L (2015) Physical features, phenolic compounds, betalains, and total antioxidant capacity of coloured quinoa seeds (*Chenopodium quinoa* Willd.) from Peruvian Altiplano. Food Chem 183:83–90

Ballabio D, Consonni V (2013) Classification tools in chemistry. part 1: linear models. PLS-DA. Anal Methods 5:3790

Ballabio D, Grisoni F, Todeschini R (2018) Multivariate comparison of classification performance measures. Chemometr Intell Lab Syst 174:33–44

Barth A (2007) Infrared spectroscopy of proteins. Biochimica et Biophysica Acta Bioenerg 1767:1073–1101

Bazile D, Baudron F (2015) The dynamics of the global expansion of quinoa growing in view of its high biodiversity, Chapter 1.4. In: FAO & CIRAD. State of the art report of Quinoa in the world in 2013, pp 42–55

Bhargava A, Shukla S, Rajan A, Ohri D (2007) Genetic diversity for morphological and quality traits in quinoa (*Chenopodium quinoa* Willd.) germplasm. Genet Resour Crop Evol 54:167–173

Capron I, Robert P, Colonna P, Brogly M, Planchot V (2007) Starch in rubbery and glassy states by FTIR spectroscopy. Carbohyd Polym 68:249–259

Di Rienzo JA, Casanoves F, Balzarini MG, Gonzalez L, Tablada M, Robledo CW (2011) InfoStat, versión 2011. Grupo InfoStat, Facultad de Ciencias Agropecuarias, Universidad Nacional de Córdoba, Argentina

Encina-Zelada C, Cadavez V, Pereda J, Gómez-Pando L, Salvá-Ruíz B, Teixeira JA, Ibañez M, Liland KH, Gonzales-Barron U (2017) Estimation of composition of quinoa (*Chenopodium quinoa* Willd.) grains by near-infrared transmission spectroscopy. LWT Food Sci Technol 79:126–134

Gislum R, Micklander E, Nielsen J (2004) Quantification of nitrogen concentration in perennial ryegrass and red fescue using near-infrared reflectance spectroscopy (NIRS) and chemometrics. Field Crops Res 88:269–277

González Martín MI, Wells Moncada G, Fischer S, Escudero O (2014) Chemical characteristics and mineral composition of quinoa by near-infrared spectroscopy. J Sci Food Agric 94:876–881

González-Muñoz A, Montero B, Enrione J, Matiacevich S (2016) Rapid prediction of moisture content of quinoa (*Chenopodium quinoa* Willd.) flour by Fourier transform infrared (FTIR) spectroscopy. J Cereal Sci 71:246–249

Guzman-Ortiz FA, Hernández-Sánchez H, Yee-Madeira H, San Martín-Martínez E, Robles-Ramírez MC, Rojas-López M, Berríos JJ, Mora-Escobedo M (2014) Physico-chemical, nutritional and infrared spectroscopy evaluation of an optimized soybean/corn flour extrudate. J Food Sci Technol 52:4066–4077

Jarvis DE, Ho YS, Lightfoot DJ, Schmöckel SM, Li B, Borm TJA, Ohyanagi H, Mineta K, Michell CT, Saber N, Kharbatia NM, Rupper RR, Sharp AR, Dally N, Boughton BA, Woo YH, Gao G, Schijlen EGWM, Guo X, Momin AA, Negrão S, Al-Balibi S, Gehring C, Roessner U, Jung C, Murphy K, Arold ST, Gojobori T, van der Linden CG, van Loo EN, Jellen EN, Maughan PJ, Tester M (2017) The genome of *Chenopodium quinoa*. Nature 542:307–312

Jellen EN, Maughan PJ, Fuentes F, Kolano BA (2015) Botany, phylogeny and evolution, Chapter 1.1. In: FAO & CIRAD. State of the art report of Quinoa in the world in 2013, pp 12–23

Johnson RA, Wichern DW (2002) Applied multivariate statistical analysis. Prentice Hall, NJ

Jolliffe IT (2002) Principal component analysis, 2nd edn. Springer, New York

Kaufman L, Rousseeuw PJ (1987) Statistical data analysis based on the L1 norm. In: Dodge Y (ed) Clustering by means of medoids. North-Holland, Amsterdam, pp 405–416

Kim Y, Kays SE (2009) Near-infrared (NIR) prediction of trans-fatty acids in ground cereal foods. J Agric Food Chem 57:8187–8193

Kizil R, Irudayaraj J, Seetharaman K (2002) Characterization of irradiated starches by using FT-Raman and FTIR spectroscopy. J Agric Food Chem 50:3912–3918

Li H, He J, Li F, Zhang Z, Li R, Su J, Zhang J, Yang B (2015) Application of NIR and MIR spectroscopy for rapid determination of antioxidant activity of Radix Scutellariae from different geographical regions. Phytochem Anal 27:73–80

Liutho M, Mercado G, Aruquipa R (2016) Climate change, quinoa production and farmers adaptation capacity in the Bolivian Altiplan. Revista de Investigación e Innovación Agropecuaria y de Recursos Naturales 3:166–178

Lohumi S, Lee S, Lee H, Cho BK (2015) A review of vibrational spectroscopic techniques for the detection of food authenticity and adulteration. Trends Food Sci Technol 46:85–98

Luna AS, Pinho JSA, Machado LC (2016) Discrimination of adulterants in UHT milk samples by NIRS coupled with

supervision discrimination techniques. Anal Methods 8:7204–7208
Miralbés C (2008) Discrimination of European wheat varieties using near infrared reflectance spectroscopy. Anal Nutr Clin Methods 106:386–389
Nascimento AC, Mota C, Coelho I, Gueifão S, Santos N, Matos AS, Gimenez A, Lobo M, Samman N, Castanheira I (2014) Characterization of nutrient profile of quinoa (*Chenopodium quinoa*), amaranth (*Amaranthus caudatus*), and purple corn (*Zea mays* L.) consumed in the North of Argentina: proximates, minerals and trace elements. Food Chem 148:420–426
Pojić M, Mastilović J, Pestorić M, Radusin T (2008) The ensuring of measurements for cereal quality determination. Food Process Qual Saf 35:11–18
Roa DF, Santagapita PR, Buera MP, Tolaba MP (2014) Ball milling of Amaranth starch-enriched fraction. Changes on particle size, starch crystallinity, and functionality as a function of milling energy. Food Bioprocess Technol 7:2723–2731
Ruiz KB, Biondi S, Oses R, Acuña-Rodríguez IS, Antognoni F, Martinez-Mosqueira EA, Coulibaly A, Canahua-Murillo A, Pinto M, Zurita-Silva A, Bazile D, Jacobsen SE, Molina-Montenegro MA (2014) Quinoa biodiversity and sustainability for food security under climate change. A review. Agron Sustain Dev 34:349–359
Tang Y, Li X, Zhang B, Chen PX, Liu R, Tsao R (2015) Characterisation of phenolics, betanins and antioxidant activities on the seeds of three *Chenopodium quinoa* Willd. Genotypes Food Chem 166:380–388
Van den Berg F, Lyndgaard CB, Sørensen KM, Engelsen SB (2013) Process analytical technology in the food industry. Trends Food Sci Technol 31:27–35
Vanden Branden K, Hubert M (2005) Robust classification in high dimensions based on the SIMCA method. Chemometr Intell Lab Syst 79(1–2):10–21
Warren FJ, Gidley MJ, Flanagan BM (2016) Infrared spectroscopy as a tool to characterize starch ordered structure—a joint FTIR-ATR, NMR, XRD and DSC study. Carbohyd Polym 139:35–42
Ye XP, Liu L, Hayes D, Womac A, Hong K, Sokhansanj S (2008) Fast classification and compositional analysis of cornstover fractions using Fourier transform near-infrared techniques. Biores Technol 99:7323–7332
Ziegler JU, Leitenberger M, Longin CFH, Würschum T, Carle R, Schweiggert RM (2016) Near-infrared reflectance spectroscopy for the rapid discrimination of kernels and flours of different wheat species. J Food Compos Anal 51:30–36